Multifractal analysis of seismicity of the Himalayan region

S. S. Teotia*, K. N. Khattri and P. K. Roy†**

*Department of Geophysics, Kurukshetra University, Kurukshetra 136 119, India
**Wadia Institute of Himalayan Geology, Dehradun 248 001, India
†Geodata Processing and Int. Centre, ONGC, Dehradun 248 195, India

Most fractal systems in nature are heterogeneous. For such fractals, a unique fractal dimension is insufficient to characterize them and the same differs depending upon the method used to estimate it. Such fractals are called multifractal and are characterized by the generalized dimension D_q. The generalized dimension D_q and D_q spectra of the spatial distribution of earthquake epicenters in the Himalayan region are studied for the time series having a window of 1964 to 1993. In general, the value of D_q is larger for low values of the parameter q. The rate of decrease (slope) of D_q spectra have been found to be associated with the change in seismicity structure in the region. Steep slopes in the D_q spectra have been found to be associated with high rates of energy release and the gentle slopes correspond to low rates of energy release in the region.

FRACTURES exhibit a fractal structure over a wide range of the fracture scale, i.e. from the scales of microfractures to megafaults[1–5]. In such systems, the number of fractures that are larger than a specified size are related by a power law to the size. The physical laws governing the fractal structures are scale invariant in nature. Since the occurrence of earthquakes is causally related to the size of fractures, they also have fractal structures in their space, time, and magnitude distributions[6–13]. The fractal structures may be homogeneous or have multiscaling. The fractal sets having multiscaling are heterogeneous and are called multifractal sets. Most fractals in nature are known to be heterogeneous. Such fractals are characterized by generalized dimension D_q. Recent studies have shown that many natural phenomena such as the spatial distribution of earthquakes, fluid turbulence are heterogeneous multifractals[14–20]. The heterogeneity and multiscaling of fractal structure of spatial distribution of earthquakes in a region is related to the heterogeneity in the distribution of the seismicity. A number of studies have been made to investigate the temporal variation of heterogeneity in seismicity using multifractal analysis in various seismic regions[20–22]. Here we report on a similar investigation for the Himalaya.

This change in spatial pattern of earthquakes is reflected in the generalized dimension D_q or D_q spectra of the seismicity. Therefore, the study of temporal variation in D_q and D_q spectra may be used to study the changes in the seismicity structure before and after the occurrence of large earthquakes, which may prove to be of value in forecasting of such events. Accordingly Hirabayashi *et al.*[20] have done the multifractal analysis of seismicity of the regions of Japan, California and Greece using fixed mass and fixed radius methods. Hirata and Imoto[21] have performed multifractal analysis of microearthquake data of Kanto region using correlation integral method. Li *et al.*[22] have performed the multifractal analysis of spatial distribution of earthquakes of Tanshan region ($M_l > 1.8$) using extended Grassberger–Procraccia method of D_q estimation. These studies have noted changes in the temporal characteristic of the generalized dimension D_q and D_q spectra which are associated with the occurrence of some large earthquakes in these regions. This question, however, needs further investigation, particularly in different tectonic domains of the world. In the present study we investigate the temporal behaviour of generalized dimension D_q as well as D_q spectra for earthquakes in the Himalaya for the period 1964–93 to see if they can serve as a precursory measure.

Data analysis

The time window for analysis was chosen to be 1964 to 1993 and the USGS earthquake catalogue for the Himalaya for this period was used for the multifractal analysis. The earthquakes for the period under investigation are shown in Figure 1. The stepped box shows the outline of the zone taken to approximate the Himalaya. The completeness of the catalogue was verified using the procedure discussed in ref. 23 and it is found to be complete for magnitude threshold of $m_b \geq 4.5$. Under the assumption that geological processes are steady over historical time and the observation capabilities are steady over the time window under consideration for $m_b \geq 4.5$, the temporal changes in the frequency of earthquakes may be attributed to the aftershocks of the larger earthquakes and to local temporal variations in seismicity.

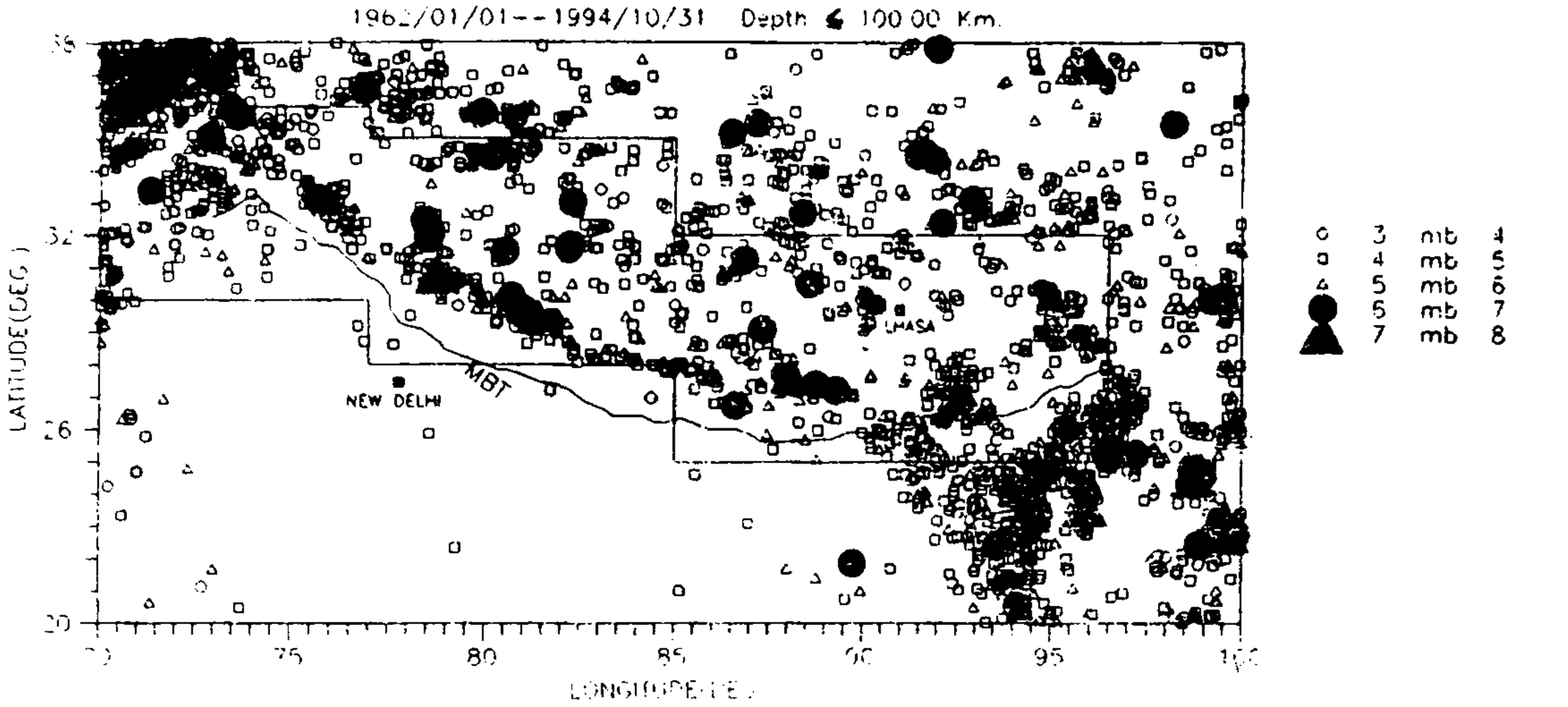

Figure 1. The seismicity of India and its adjoining areas. The main boundary thrust (MBT) is also shown.

Analytical framework for the analysis

The available methods for calculating D_q are the box-counting method[24–27], the fixed-radius method[28] and the fixed-mass method[29,30]. These methods work well provided the number of data points is very large[28–30]. The extended Grassberger and Procaccia method[31,32] is used in our analysis, which can recover the dimension from a time series. It is described as follows:

$$\log C_q(r) = D_q \log r \ (r \to 0), \tag{1}$$

$$C_q(r) = \text{Lim } r \to \left\{ (1/N) \sum_{j=1}^{N} \left[(1/N) \sum_{\substack{i=1 \\ i \neq j}}^{N} H(r - X_i - X_j) \right]^{q-1} \right\}$$

$$\times 1/q - 1, \tag{2}$$

where r is the scaling radius, N is the total number of data points within a search region in a certain time interval (also called the sample volume); X_i is the epicentral location (given in latitude and longitude) of the ith event, X_j is the epicentre (given in latitude and longitude) of the jth event, $C_q(r)$ is the qth order integral and $H(.)$ is the Heaviside step function.

In the procedure for estimating D_q spectra as a function of time, a time series of earthquake epicenters has to be formed and divided into sub-series (subsets). Let set $\{X_i, M_i\}_{i=1}^{N}$ be a complete set of earthquakes occurring in time period 1964–1993, and M_i the magnitude of an earthquake occurring at time t_i. Thus the earthquakes constitute a time series of N elements. We consider this time series as the original data set.

In the present case the original data set is divided into 21 subsets. Each subset consists of 300 events with an overlap of 260 events. The subsets and their corresponding time periods are given in Table 1. $C_q(r)$ is calculated using equation (2) for the epicentral distribution X_i of

Table 1. The subsets and their corresponding time periods along with the number of large events occurring in different magnitude ranges

Subset event	Time period (years)	$6.0 \leq m_b < 6.5$ (No. of events)	$6.5 \leq m_b < 7.0$ (No. of events)
1–300	1963.068–1973.980	6	1
41–340	1964.766–1974.482	6	1
81–380	1965.697–1975.699	4	1
121–420	1967.113–1976.633	4	1
161–460	1968.499–1977.883	4	1
201–500	1971.079–1979.246	4	.
241–540	1973.738–1979.883	4	.
281–580	1973.202–1980.858	6	.
321–620	1974.085–1981.592	4	.
361–660	1974.947–1983.066	4	.
401–700	1976.208–1983.874	4	.
441–740	1977.146–1984.555	4	.
481–780	1978.933–1985.394	4	.
521–820	1979.646–1986.313	3	.
561–860	1980.633–1987.280	2	.
601–900	1981.135–1988.189	1	1
641–940	1982.074–1989.678	1	1
681–980	1983.363–1990.555	1	1
721–1020	1984.316–1991.305	1	2
761–1060	1984.958–1992.124	2	2
801–1099	1985.694–1993.00	2	2

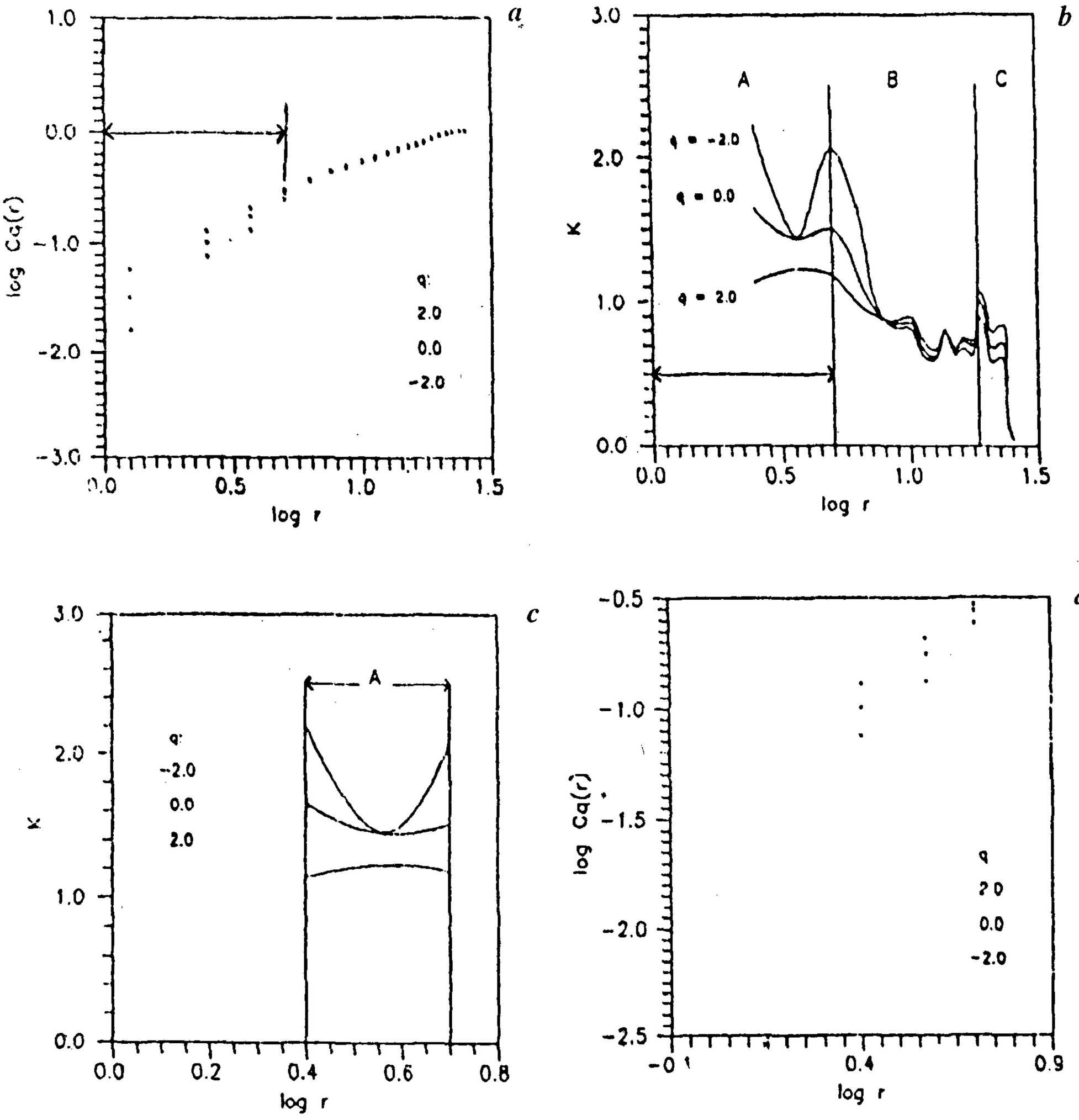

Figure 2. Selection of scaling region for Himalaya earthquakes, $N = 300$. *a*, Log r versus log $C_q(r)$ for three values of q; *b*, Log r versus K curve of (*a*). *c*, Log r versus K of region A which is shown in (*b*); *d*, Log r versus Log $C_q(r)$ curve of region A which is shown in (*c*).

the subset. The distance r between two events is calculated by using spherical triangle[33]. For epicentral distribution having a fractal structure, the following power law relationship is obtained in the scaling region.

$$C_q(r) \sim r^{D_q}.$$

An appropriate scaling region has to be estimated before the computation of the generalized dimension D_q. The scaling region is a linear segment in the graph of log r versus log $C_q(r)$. The scaling region may be characterized by the circular boundary defined by scaling radius around epicentre. We use the method of Li *et al.*[22] to determine the scaling region in Himalaya. Three point curves for $q = 2.0$, 0.0, –2.0 respectively are shown in Figure 2*a* which are studied for the selection of the scaling region. There may be two or more linear segments in each curve. It is known that slopes of adjacent points in the graph will be constant when these points lie on a linear segment. The graph of log r versus K (K is the slope of adjacent points of the graph of log r versus log $C_q(r)$ is shown in Figure 2*b*. A, B and C are the three possible regions which are separated by the cusps. The scaling region corresponds to the range in r for which the variation in slope K is a minimum. The

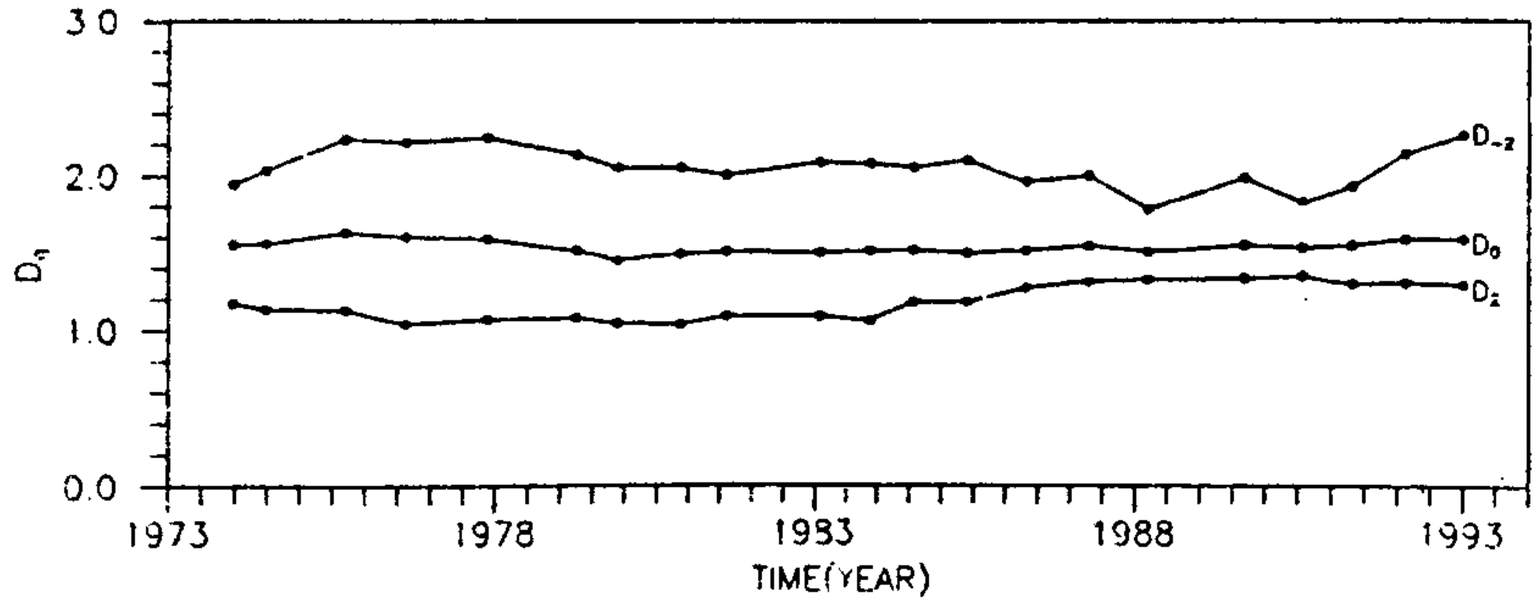

Figure 3. The temporal change of generalized dimension D_q for q, −2.0, 0.0, 2.0 in order from top to bottom for the epicenter distribution.

variation in K for $r(0.0°, 5.0°)$ is a minimum which corresponds to the region A. There is approximately one linear segment A in each curve for different values of q in the graph of log r versus log $C_q(r)$.

The region A has therefore been selected to calculate generalized dimension D_q. The range of r in region A is r_0 . Thus the scaling region will be characterized by the circular boundary of radius r_0. The scaling parameter within the boundary will be different from the scaling parameter outside the boundary. The value of scaling radius r_0 in region A is about 5°, the maximum distance of two points in the earthquake data in Himalaya region is $r_{max} \sim 25°$, so r_0/r_{max} equals approximately (1/5). This implies that the boundary effect[22] will be present if the scaling radius r_0 is larger than $(1/5)r_{max}$. The reference regions B and C lie outside the scaling region having significant deviations from linearity. The generalized dimension D_q is obtained by getting the slope of the linear segment which lies in the scaling region. The D_q values for the epicentral distribution of all the 21 subsets are calculated in the same scaling range.

Results and discussion

The generalized dimension D_q is calculated for the time series comprising 21 subsets of earthquakes following the procedure outlined above. The standard deviations of the estimates of D_q are less than 10% and are generally smaller for larger values of q. The D_q for negative q is considerably more sensitive to the changes in the fractal structure of the earthquakes than the D_q for $q > +2$. This is exemplified by the higher slopes of the D_q curves for $q < 2$.

Figure 3 shows the temporal variations of D_q for three different values of q(−2, 0 and 2) from the year 1964 to 1993. The D_q values for each subset are plotted at the time where the last earthquake entered the subset. The first subset of 300 earthquakes starts from 1963.068 years and ends at 1973.980 years. Thus the D_q value evaluated for this subset is plotted on the time axis at 1973.980 years. The temporal changes observed in D_{-2} are larger and rough as compared to the variations in the other two dimensions D_0 and D_2. Among the three dimensions, D_0 has the least variation, to the point of being almost flat. Furthermore, the changes in D_2 and D_{-2} are in the opposite directions. This feature signifies that as the clustering of the earthquakes increases, i.e. D_2 decreases, the D_{-2} increases which represents an increase in the patches having little or no earthquakes. Thus in the time period 1964–1983, increased levels of clustering of the earthquakes would occur, whereas in the period 1983–1993, the D_2 assumes larger values and would therefore characterize decreased levels of clustering. Accordingly, the multifractal characteristics of the earthquakes in Himalaya are changing with time.

The value of D_0 ranges from 1.45 to 1.60 in the total time period (1964–1993). Sadovskiy *et al.*[11] obtained a value of 1.5 for D_0 for a catalogue of world-wide earthquakes. Thus our estimates for D_0 in the Himalaya are close to the above value of global data set. The variation in D_2 is 1.0–1.3 and D_{-2} is 1.78–2.26. A lower value of D_2 obtained for the Himalaya shows that the fracture distributions are tending to fill a two-dimensional space through primary as well as secondary faulting. However, the low value of fractal dimension corresponds to a higher percentage of release of earthquake energy through primary faulting and the rest on the fractal distribution of sub-faults[34,35]. In the Himalaya primary, the faulting is considered to be due to the basement thrust fault[36] on which the larger magnitude earthquakes occur. This is a north dipping (~6°) surface at a depth of about 15–20 km. It constitutes a megathrust extending along the entire Himalaya for about 2,400 km and having an average width of about 80 km. Thus the low value of D_2 indicates that the seismic activity is mainly due to the primary faulting over the boundary thrust fault in the region. As D_2 has a fairly constant value of 1.0 in the

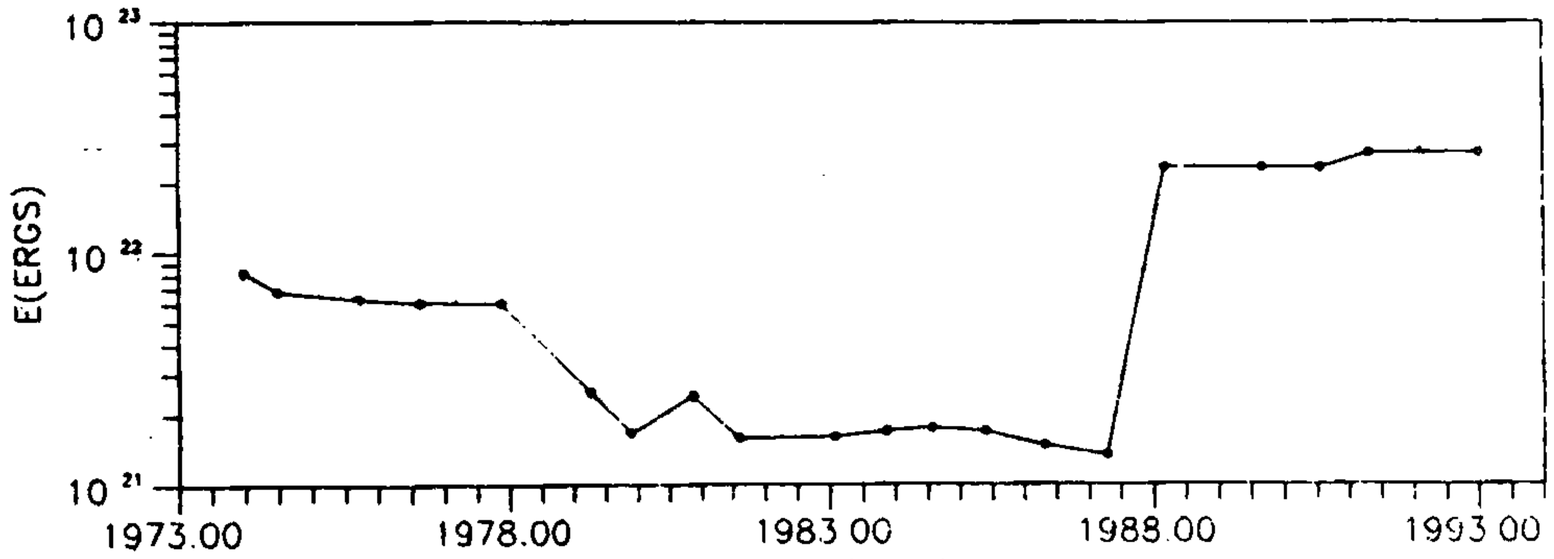

Figure 4. The temporal variation of energy released in various subsets.

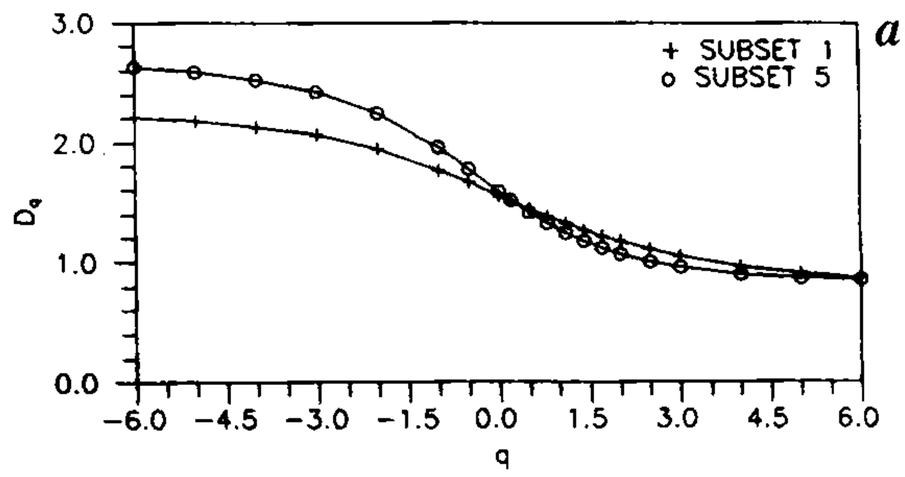

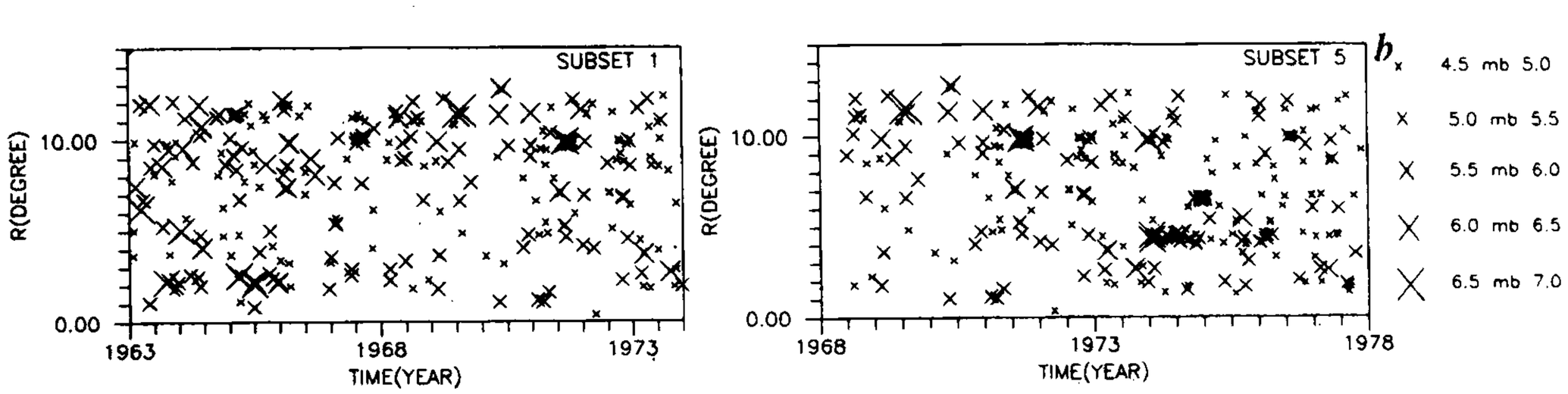

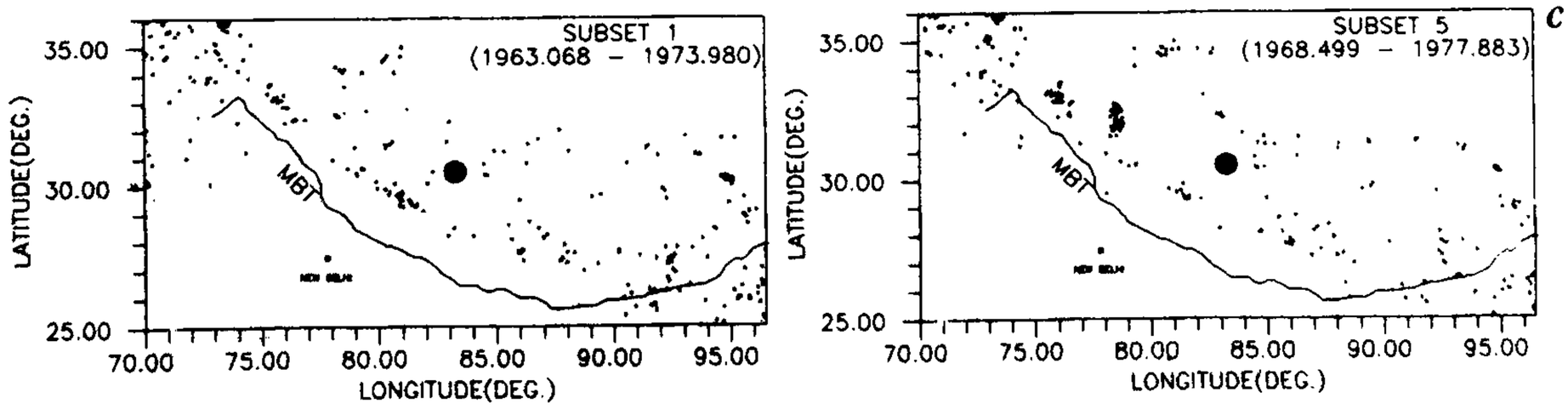

Figure 5. Multifractal analysis of epicenter distribution of earthquakes occurring in subset 1 and subset 5. *a*, The D_q spectra of subset 1 and subset 5; *b*, Spatio-temporal pattern of seismicity in (R–T) domain, the distance R is calculated for all earthquakes in subsets from the reference point shown by solid circle in (*c*). *c*, The epicentral distribution of earthquakes occurring in different time windows in subset 1 and subset 5.

period 1973–1983, it may be interpreted as indicating the seismic activity in this period to be dominated by primary faulting. On the other hand, D_2 attains higher value of about 1.4 in the period 1983–1993 suggestive of a tendency for the earthquakes to fill a 2-dimensional space.

The seismic energy distribution in various subsets is shown in Figure 4. One notices three distinct levels of energy, viz. from 1973 to 1978; 1978 to 1988 and 1988 to 1993. The shapes of the curves in each of these periods are similar. The levels are determined by the larger events, viz. the 1975 M_s 6.8 earthquake, the M_s 7.2 1988 Bihar earthquake and the M_s 7 1991 Uttarkashi earthquake. We would like to recognize if these events caused corresponding anomalies in the D_q curves. The period of 1988–1993 shows a very significant increase in D_{-2}, and a weaker decrease in D_2. This feature signifies increased level of clustering of earthquakes. Similarly where M_s 6.8 event occurred in the beginning of the period 1973 we observe a similar pattern as above. Occurrence of clustering associated with larger events has been observed in other studies in California, Japan and China[20–22]. We may interpret a general increase of clustering during periods of larger earthquakes.

D_q spectra of the subsets

The D_q versus q curve is termed as D_q spectra. We r discuss the features of typical D_q spectra for the t time zones discussed above. The D_q spectra is a decr ing function of q. The shape of the D_q spectra is pected to be diagnostic of the temporal changes seismicity patterns before large earthquakes. The sl of the D_q spectra becomes gentle for the extended di bution of earthquakes and it becomes steep for the c of concentrated distribution of earthquakes. As be large earthquakes clustering of earthquakes may oc leading to a steep D_q spectra which may serve a pre sory anomaly[20–22]. Thus seismicity distributions h evolutionary nature which may form distinctive patte For studying the nature of evolving seismicity patte in addition to the D_q spectra, we also plot the spa distribution of earthquake epicenters and the graph distance (R) of epicenters from a reference point and

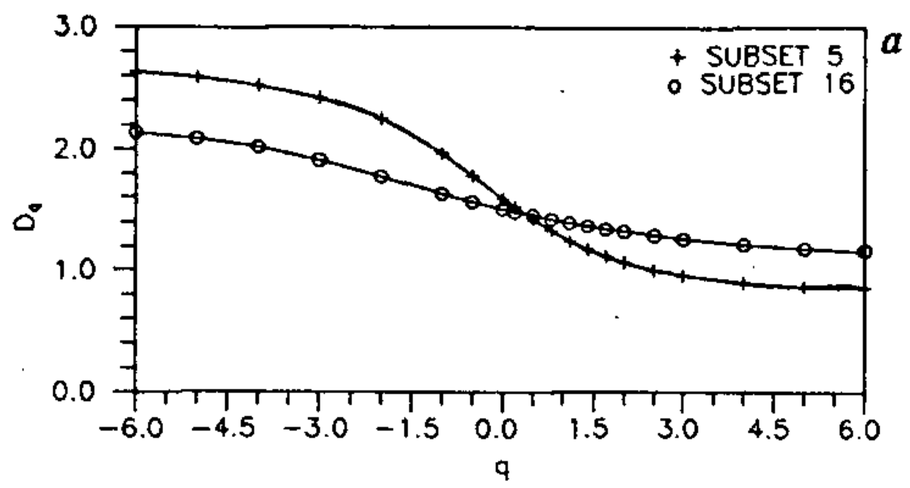

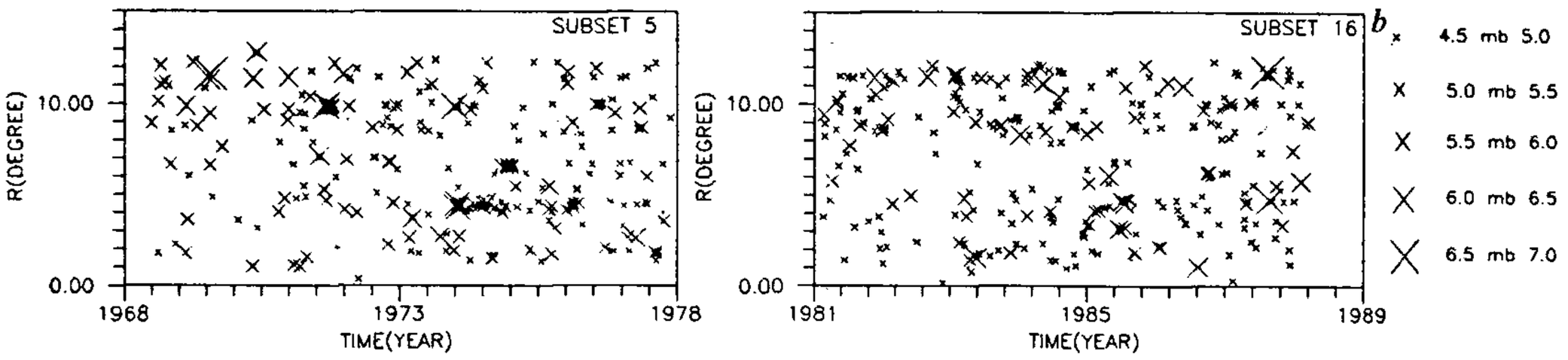

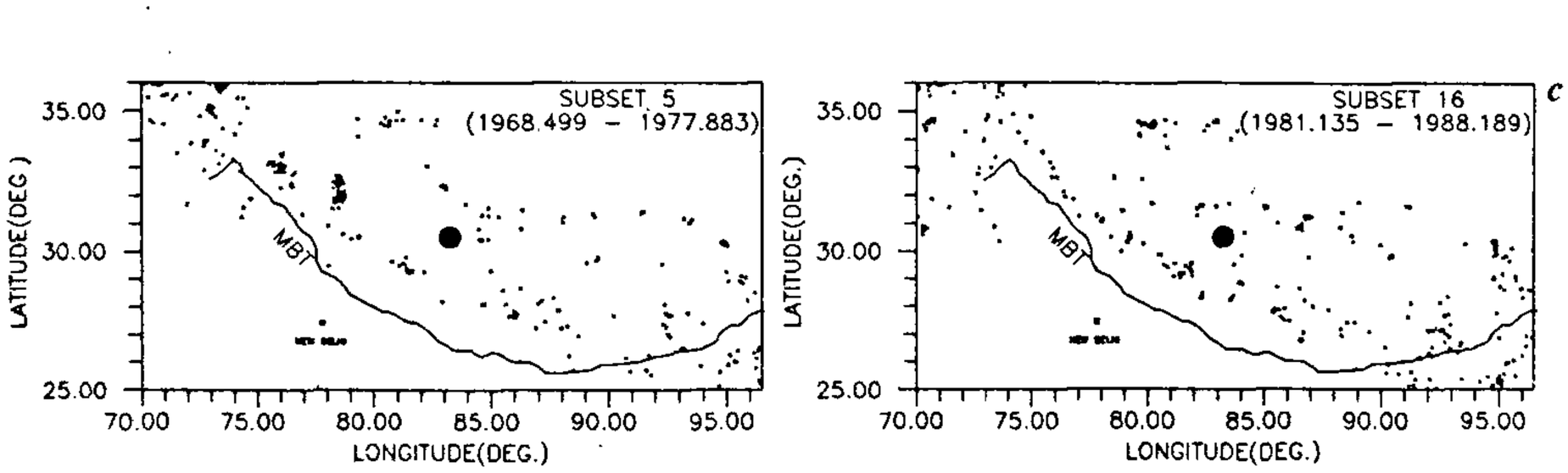

Figure 6. *a*, The D_q spectra of subset 5 and subset 16; *b*, Spatio-temporal pattern of seismicity in (R–T) domain; *c*, The epicentral distribution of earthquakes occurring in different time windows in subset 5 and subset 16.

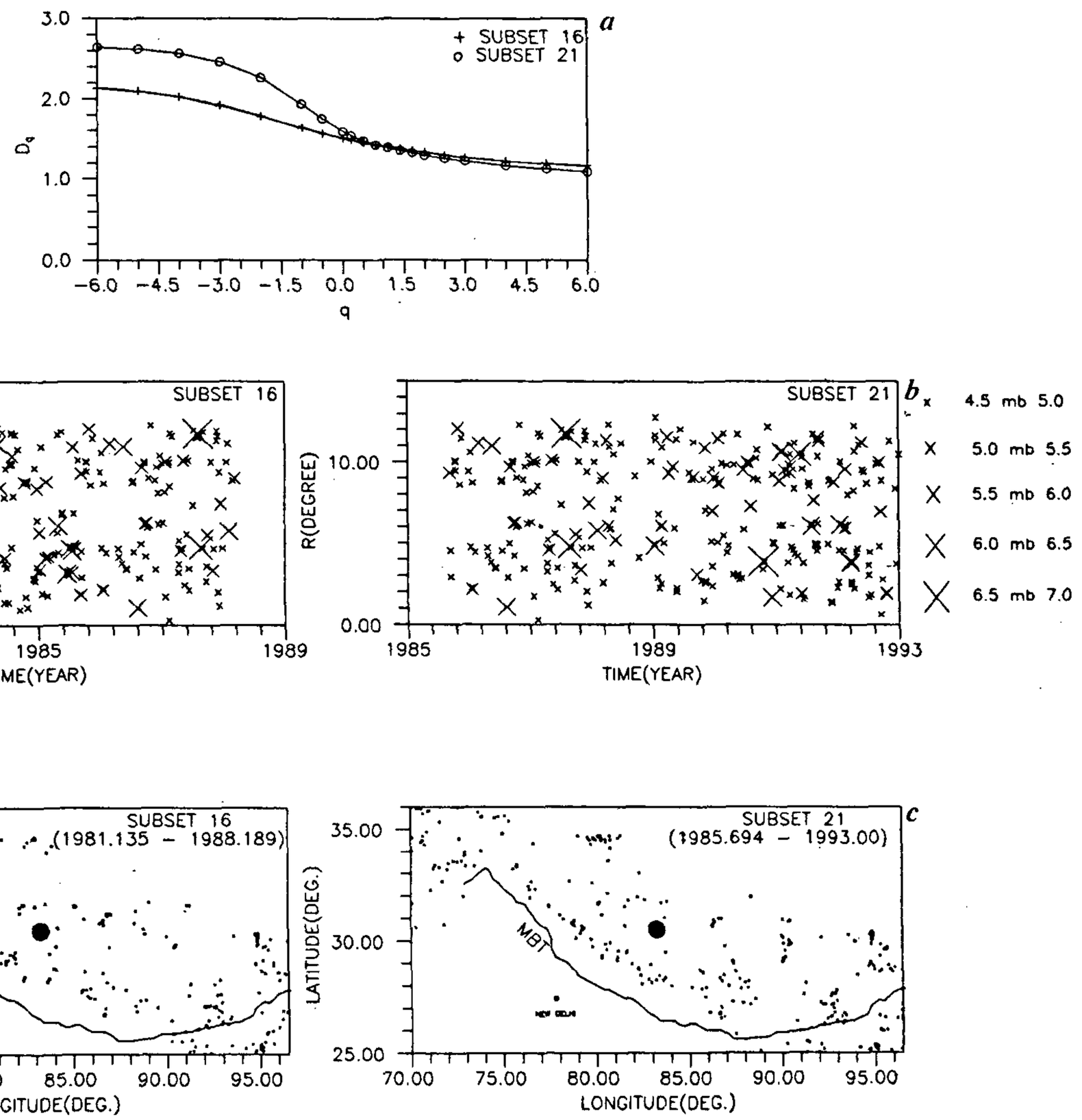

Figure 7. *a*, The D_q spectra of subset 16 and subset 21; *b*, Spatio-temporal pattern of seismicity in (R–T) domain; *c*, The epicentral distribution of earthquakes occurring in different time windows in subset 16 and subset 21.

corresponding time of occurrence (T). Figure 5 *a* shows the D_q spectra in the first time zone, i.e. 1973–1978. The slope of D_q spectra for subset 5 in this time zone is steeper than for subset 1. This indicates that an increase in the clustering and gaps is occurring progressively with time. The corresponding display of these features in the epicentral distribution is shown in Figure 5 *b* and in the R–T domain in Figure 5 *c*. The epicentral plot for subset 5 shows a discernible increase in clustering as compared to the similar plot for subset 1. Similarly the R–T plot indicates a similar increase in clustering in the case of subset 5.

For the second time period 1978–1988, we compare the patterns in D_q spectra, R–T plot and epicentral maps for subset 5 and subset 16. In this case we observe that the pattern is moving from a state of clustering to declustering. The slope of D_q spectra moves from a steep shape for subset 5 to a gentle slope for subset 16. The corresponding feature may be seen in the R–T and epicentral plots (see Figures 6 *a–c*). Similarly for the third time zone (1988–1993) we notice the seismicity pattern moving from a state of dispersed structure to clustered structure. The slope of D_q spectra changes from a gentle shape for subset 16 to a steep shape for subset 21. Corresponding features may be seen in R–T and epicentral plots (see Figures 7 *a–c*).

Conclusions

The present study shows the multifractal nature of seismicity in the Himalaya region. The multifractal characteristics vary with time. The heterogeneity of the multifractal is related to larger magnitude earthquakes. However, the magnitude threshold of $m_b \geq 4.5$ and relatively small time window constrain the resolution of the analysis. But as there is a general correlation of the features of clustering as indicated by D_q with the large magnitude earthquakes, it holds promise for serving as precursory parameter for earthquake data sets having lower magnitude threshold and larger time window. The

correspondence between the energy released and the D_q spectra may be used in seismic hazard studies.

1. Brown, S. R. and Scholz, C. H., *J. Geophys. Res.*, 1985, **90**, 12575–12582.
2. Scholz, C. H. and Aviles, C. A., in *Earthquake Source Mechanics* (eds Das, S., Boatwright, J. and Scholz, C. H.), Maurice Ewing Ser. 6, American Geophysical Union, Washington D.C., 1986, pp. 147–155.
3. Okubo, P. G. and Aki, K., *J. Geophys. Res.*, 1987, **92**, 345–355.
4. Sammis, C. G. and Biegel, R. L, *Pageoph*, 1989, **131**, 255–271.
5. Hirata, T., *Pageoph*, 1989, **131**, 157–170.
6. Aki, K., *An International Review* (eds Simpson, D. W. and Richards, P. G.), Maurice Ewing Ser 4, AGU, Washington, DC, 1981, pp. 566–574.
7. King, G., *Pageoph*, 1983, **121**, 761–815.
8. Kagan, Y. Y. and Knopoff, L., *Geophys. J. R. Astron. Soc.*, 1978, **55**, 67–86.
9. Kagan, Y. T. and Knopoff, L., *Geophys. J. R. Astron. Soc.*, 1980, **62**, 303–320.
10. Ogata, Y., *J. Am. Stat. Assoc.*, 1988, **83**, 401.
11. Sadovskiy, M. A., Golubeva, T. V., Pisarenko, V. F. and Shnirman, M. G., *Izv. Acad. Sci. USSR Phys.*, (Solid Earth Engl. Transl.), 1984, **20**, 87–96.
12. Hirata, T., *J. Geophys. Res.*, 1989, **94**, 7507–7514.
13. Hirata, T., Satoh, T. and Ito, K., *Geophys. J. R. Astron. Soc.*, 1987, **90**, 369–374.
14. Frisch, U., Sulem, P. L. and Nelkin, M., *J. Fluid Mech.*, 1978, **87**, 719–736.
15. Stanley, H. E. and Meakin, P., *Nature*, 1988, **335**, 405–409.
16. Mandelbrot, B. B., *J. Fluid Mech.*, 1974, **62**, 331–358.
17. Mandelbrot, B. B., in Proceedings of the 13th IUPAP Conference on Statistical Physics (eds Cabib, E., Kuper, C. G. and Reiss, I.), Hilger, Bristol, 1978.
18. Frisch, U. and Parisi, G., in *Turbulence and Predictability in Geophysical Fluid Dynamics and Climate Dynamics* (eds Ghil, M. *et al.*), North Holland, Amsterdam, 1985, p. 84.
19. Mendelbrot, B. B., *Pageoph*, 1989, **131**, 5–42.
20. Hirabayashi, T., Ito, K. and Yoshii, T., *Pageoph*, 1992, **138**, 591–610.
21. Hirata, T. and Imoto, M., *Geophys. J. Int.*, 1991, **107**, 155–162.
22. Dongsheng, Li., Zhaobi, Z. and Binghong, W., *Tectonophysics*, 1994, **223**, 91–97.
23. Khattri, K. N., Rogers, A. M. and Perkins, D. M., *Bull. ISET*, 1983, **20**, 1–22.
24. Grassberger, P., *Phys. Lett. Ser. A*, 1983, **97**, 227–230.
25. Hentchel, H. G. and Procraccia, I., *Physica Ser. D*, 1983, **8**, 435–455.
26. Halsey, T. C., Kadanoff, L. P., Procraccia, I. and Shraiman, B. I., *Phys. Rev. A*, 1986, **33**, 1141–1151.
27. Greenside, H. S, Wolf, A., Swift, J. and Pignataro, T., *Phys. Rev.*, 1982, **A25**, 3453–3459.
28. Jensen, M. H., Kadanoff, L. P., Libchaber, A., Procaccia, I. and Stavans, J., *Phys. Rev. Lett.*, 1985, **55**, 2798–2801.
29. Grassberger, P., Baddii, R. and Politi, A., *J. Stat. Phys.*, 1988, **51**, 135–178.
30. Badii, R. and Broggi, G., *Phys. Lett.*, 1988, **A131**, 339–343.
31. Grassberger, P. and Procraccia, I., *Phys. Rev. Lett.*, 1983, **50**, 346–349.
32. Pawelzik, K. and Schuster, H. G., *Phys. Rev.*, 1987, **35**, 481–484.
33. Bullen, K. E. and Bolt, B. A., *An Introduction to Theory of Seismology*, Cambridge University Press, New York, 1985.
34. Turcotte, D. L., *Pageoph*, 1986, **132**, 361–369.
35. Khattri, K. N., *Curr. Sci.*, 1995, **69**, 361–366.
36. Seeber, L. and Armbruster, J. G., *Geodynamic Series 3*, Am. Geophys, Union, 1981, p. 215.

ACKNOWLEDGEMENTS. Financial assistance provided by CSIR to K. N. Khattri under Scientist-Emeritus scheme is greatly acknowledged. We also thank Dinesh Kumar and Dr. Nand Lal for their help during this work.

Received 30 November 1996; revised accepted 16 June 1997